

# PROPPANT TRANSPORT

E. J. NOVOTNY

Exxon Production Research Company

## ABSTRACT

*A method is presented for predicting the transport of proppant in a fracture during a hydraulic fracturing treatment. In addition, the settling of the proppant during closure of the fracture following the treatment is considered. From the final distribution of proppant, increases in well productivity (stimulation) are calculated. The examples given illustrate that proppant settling during fracture closure can determine the success or failure of a hydraulic fracturing treatment.*

## INTRODUCTION

In hydraulic fracturing, fluid is injected into a well at a high enough rate and pressure to crack open the productive formation. When the fracture is estimated to be sufficiently wide and long, sand or some suitable propping material is injected along with additional fluid. The function of the proppant is to keep the fracture open after injection stops. The amount of production increase, or stimulation, from a hydraulic fracturing treatment depends on the conductivity and final distribution of proppant in the fracture.

While proppant is injected into the fracture, it travels along with the fluid away from the wellbore and settles downward at a rate that depends on the fluid properties and surrounding conditions. When the treatment is over, the fracture closes as fracturing fluid is lost through the permeable walls of the fracture. While this is happening, the proppant continues to settle until: 1) the proppant forms a bank at the bottom of the fracture, 2) the proppant concentration in the slurry becomes so high that it can no longer settle, or 3) the fracture closes on the slurry, trapping the proppant. Pressure measure-

ments following a treatment have indicated fracture closure in the field. Sometimes the rate of closure can determine the success or failure of the treatment. Until now, however, fracture closure has not been realistically considered in treatment design.

The prediction of proppant transport is intricate because, as the slurry travels from the wellbore, several things occur: the proppant and fluid are heated, and the formation rock is cooled. Because fluid is continuously lost to the reservoir, the proppant concentration increases and the fluid velocity decreases. The width of the fracture decreases away from the wellbore, which alters the fluid velocity. These and other factors that affect the settling velocity of the proppant and its velocity along the fracture are too numerous and complex to model adequately unless numerical computational techniques are used.

Previous research<sup>1</sup> that modeled the transport of proppant while fracturing did not model fracture closure. This paper presents a method that models the entire fracturing process, including closure. The equations for proppant settling are developed theoretically and verified experimentally. Most stimulation predictive methods assume a rectangular fracture, but in the method presented here the fracture permeability, width, and effective height can vary with fracture length. The following section discusses the importance of accurate proppant transport predictions for optimum treatment design, emphasizing fracture closure. Details of the computer model, theory, and experimental work will then be presented.

## RESULTS AND DISCUSSION

Four computer-simulated example treatments are used to illustrate the importance of accurate

---

This paper was first presented at the SPE-AIME 52nd Annual Fall Technical Conference and Exhibition, October 9-12, in Denver.

proppant transport predictions, including the effect of fracture closure. Well data specified for these examples are given in Table 1, treatment data and results are given in Table 2, and a pictorial representation of the treatments is shown in Figure 1. All four treatments used an emulsion fracturing fluid composed of 33% brine and 67% oil in which the concentration of gelling agent varied from 0.5 to 2 lb/bbl of brine. In all four treatments the injection rate was 10 BPM with a 100-bbl pad followed by 150 bbl containing 2 lb/gal of 20/40 sand and 150 bbl containing 2 lb/gal of 10/20 sand. Since fluid-loss additive (20 lb/1000 gal) was used in the fluid for all four jobs, the dynamic fracture geometries of the four treatments did not differ appreciably. However, the viscosity of the fracturing fluids differed considerably as indicated by the fluid properties in Table 2. This change in fluid properties affected the settling velocity of the proppant.

TABLE 1—WELL DATA FOR TREATMENT COMPARISON

Formation Properties:	
Reservoir Depth	10,000 ft
Fracture Gradient	0.70 psi/ft
Gross Fracture Height	60 ft
Reservoir Sand Thickness	20 ft
Porosity	0.10
Permeability	1.0 md
Reservoir Temperature	200° F
Young's Modulus	10 <sup>7</sup> psi
Well Spacing	80 acres
Reservoir Fluid Properties:	
Viscosity	2.0 cp
Density	50.00 lb/ft <sup>3</sup>
Compressibility	0.0002 psi <sup>-1</sup>
Pressure	5000 psi

In Figure 1 the simulated treatments are arranged in order of increasing gel concentration from left to right. Time increases from top to bottom, with proppant injection ending at 40 minutes. After this time, the effects shown in Figure 1 are those of the fracture closing.

In Treatment A for the first 22 minutes only 20/40 sand was injected and this settled relatively little. At 28 minutes, the 10/20 sand entered the fracture and settled faster. At the end of injection (40 minutes), the larger 10/20 mesh sand started forming a proppant bank near the wellbore. The 20/40 sand was displaced farther along the fracture and had separated from the larger 10/20 mesh sand. If the

TABLE 2—TREATMENT DATA AND RESULTS

TREATMENT	A	B	C	D
Lbs of Gelling Agent/bbl of Brine	0.5	1.0	1.5	2.0
Fluid Properties at 200° F				
K (poises)	0.81	2.65	8.53	27.0
n	0.81	0.71	0.60	0.50
Proppant Settling Velocities* (cm/sec)				
10/20 Sand	4.26	1.30	0.28	0.032
20/40 Sand	0.69	0.18	0.032	0.0027
Dynamic Fracture Length (ft)	906	852	797	739
Dynamic Fracture Width @ Wellbore (in.)	0.192	0.211	0.234	0.262
Fluid Efficiency (%)	60	62	64	67
Stimulation Ratio				
Predicted This Study	1.01	2.61	4.10	4.16
Estimated From McGuire-Sikora	1.00	2.31	4.37	4.47
Predicted If Closure Time = 0	3.68	4.00	4.10	4.16

Data Common To All Treatments:

Injection Rate	10 BPM
Injection Temperature	100° F
Pad Volume	100 BBL
First Stage	150 BBL w/2 lb/gal 20/40 Sand
Second Stage	150 BBL w/2 lb/gal 10/20 Sand
Permeability of 20/40 Sand	76 Darcies @ 5000 psi Stress
Permeability of 10/20 Sand	120 Darcies @ 5000 psi Stress

\*As predicted by Eq. (7).

fracture would close quickly at this point so that the 10/20 mesh sand would not completely settle, a stimulation ratio of about 3.7 would be obtained. As seen from Figure 1, however, the 10/20 mesh sand continued to settle and, in fact, completely settled into a proppant bank before the fracture closed at 105 minutes. As a result, the 10/20 mesh proppant settled completely beneath the productive reservoir sand interval. Studies using a three-dimensional reservoir simulator<sup>2</sup> have shown that there would be no stimulation from this treatment. Treatment A is a good example of how ignoring fracture closure can result in a poorly designed treatment.

In Treatment B, the gel concentration and viscosity were higher, so the 10/20 mesh sand settled slower and some of the net reservoir sand near the wellbore was propped when the fracture closed at 107 minutes. Had the fracture closed quickly after injection stopped, a stimulation ratio of 4.0 would have been obtained. However, about an hour was required for the fracture to close. During this time, much of the 10/20 proppant settled beneath the net reservoir sand, resulting in a stimulation ratio of only 2.6.

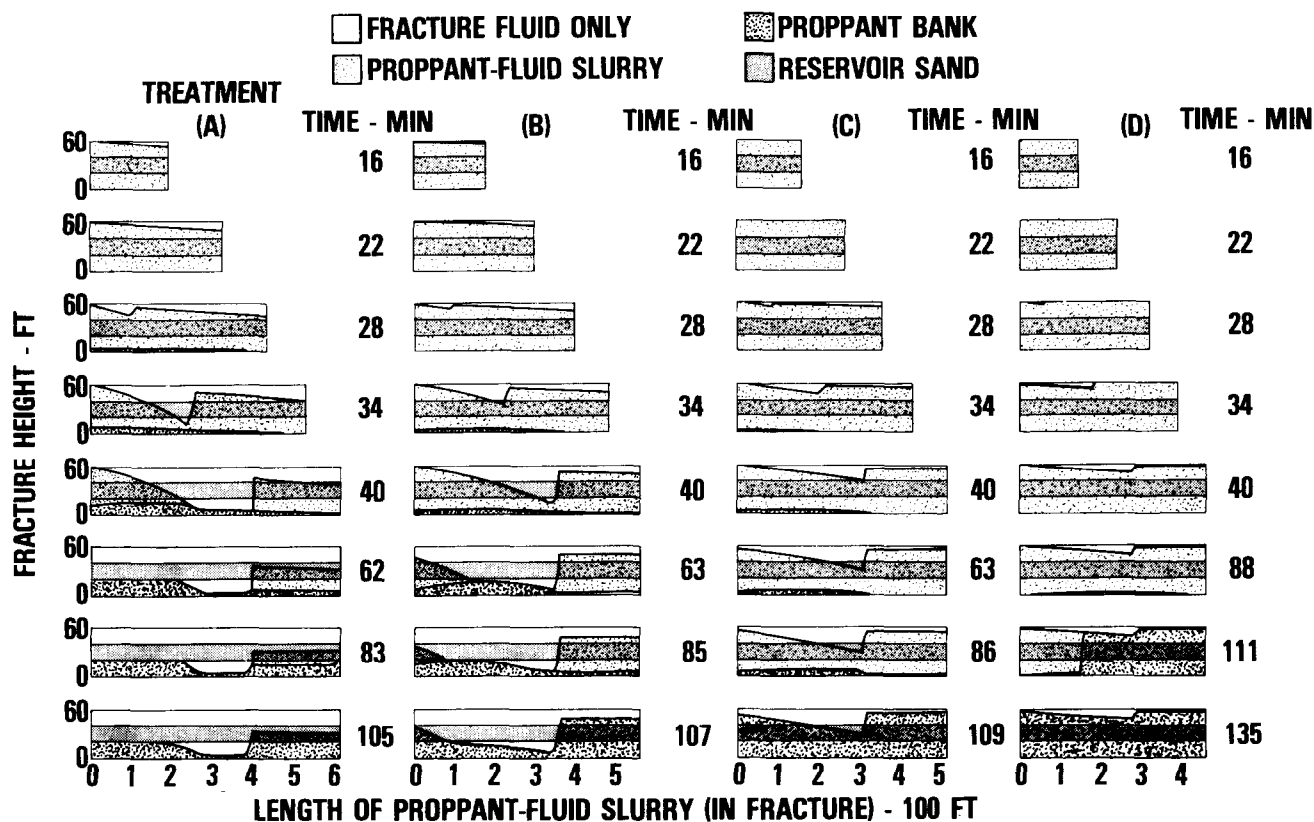


FIGURE 1—PROPPANT SLURRY BEHAVIOR DURING AND AFTER A HYDRAULIC FRACTURING TREATMENT SHOWS THE IMPORTANCE OF FRACTURE CLOSURE. DATA FOR THESE TREATMENTS ARE IN TABLES 1 AND 2.

Treatment C was an improvement over A and B. At the end of injection, the proppant slurry covered the entire net-permeable reservoir sand interval. While the fracture was closing, the proppant settled only a short distance. When the fracture was closed (at 109 minutes), the net reservoir sand was propped almost completely. The stimulation ratio was 4.1, the same result as if the fracture had closed quickly after injection stopped. This stimulation was considerably better than either of the first two treatments.

Treatment D contained the highest amount of gelling agent; when the fracture closed, even the 10/20 sand had settled only slightly. In this case, the fracture closed slower than in the previous three cases. At 111 minutes, the fracture had closed from the tip to a point 150 ft from the wellbore. During the next 24 minutes, the fracture closed the remaining distance to the wellbore. The fracture closed from the tip toward the wellbore, because at the tip of the fracture the width was narrower and the proppant concentration higher than they were closer to the wellbore. The proppant bank

completely covered the net reservoir sand (at 135 min), resulting in a 4.2 stimulation ratio (which was slightly better than treatment C).

Note that in Figure 1 the computed fracture length shown is not the dynamic fracture length but the length of the proppant-fluid slurry. Dynamic fracture lengths were anywhere from 700 to 900 ft, as shown in Table 2. This means that the proppant traveled to about 2/3 of the total fracture length. We cannot assume that even a completely suspending fluid, such as in Treatment D, carries the proppant to the end of the fracture.

The importance of fracture closure in these examples is obvious. One cannot assume that the fracture closes instantaneously at the end of proppant injection. By modeling fracture closure, treatment design can be improved and better stimulations obtained. It is also important to know accurately proppant settling velocities. For the treatments in Figure 1 there is a large difference in proppant settling velocities, as shown in Table 2. Errors of these magnitudes could mean the difference between a successful treatment, such as C

or D, and a complete or partial failure such as A or B. The effects discussed in the section on settling theory and experimentation will show that many of the factors that influence proppant settling can change settling velocity by an order of

magnitude—and sometimes several orders of magnitude.

The prediction of stimulation ratios is discussed in the Computer Model section. In Table 2, the stimulations predicted using this new method are compared with estimated stimulations from McGuire-Sikora.<sup>3</sup> For all four treatments there is good agreement between the two methods. Because McGuire-Sikora assume the propped fracture is rectangular, the fracture was estimated to be propped to that distance where the proppant bank was not directly opposite any portion of the net reservoir sand.

Fracture closure in the field, as evidenced by surface pressure data, is compared in Figure 2 with predictions from the model presented here. The solid curves show surface tubing pressures taken in the field immediately after a fracturing treatment. Up to 130 minutes after injection ceased, the pressure decreased slowly in well A because the minimum principal stress in the earth continued to squeeze the fluid in the fracture, keeping the pressure high. At 130 minutes, the pressure decreased rapidly. At this point the fracture had closed and the proppant now supported the minimum principal stress. As more fluid was lost to the formation, the pressure in the fracture and the wellbore quickly decreased. For well B, the break in the measured surface tubing pressure curve is not as graphic as in well A, but this break does occur at the original instantaneous shut-in pressure of 4600 psi.

Predictions from the computer model were fairly close to the field results for well B—the fracture was predicted to close in 100 minutes, whereas closure actually occurred in 130 minutes. Well A was predicted to close in 45 minutes, but actually closed in 130 minutes.

The field data in Figure 2 show that fracture closure can be observed, at least in these reservoirs, by monitoring surface pressure following a treatment. By insuring that the fracture is completely closed before returning the well to production, production of proppant can be mitigated. If the wells in Figure 2 had been produced prior to 130 minutes, it is likely that proppant in the near-wellbore region would have been produced and perhaps would have voided this region of the fractures. If this occurred, the fractures would close near the wellbore, resulting in poor stimulation.

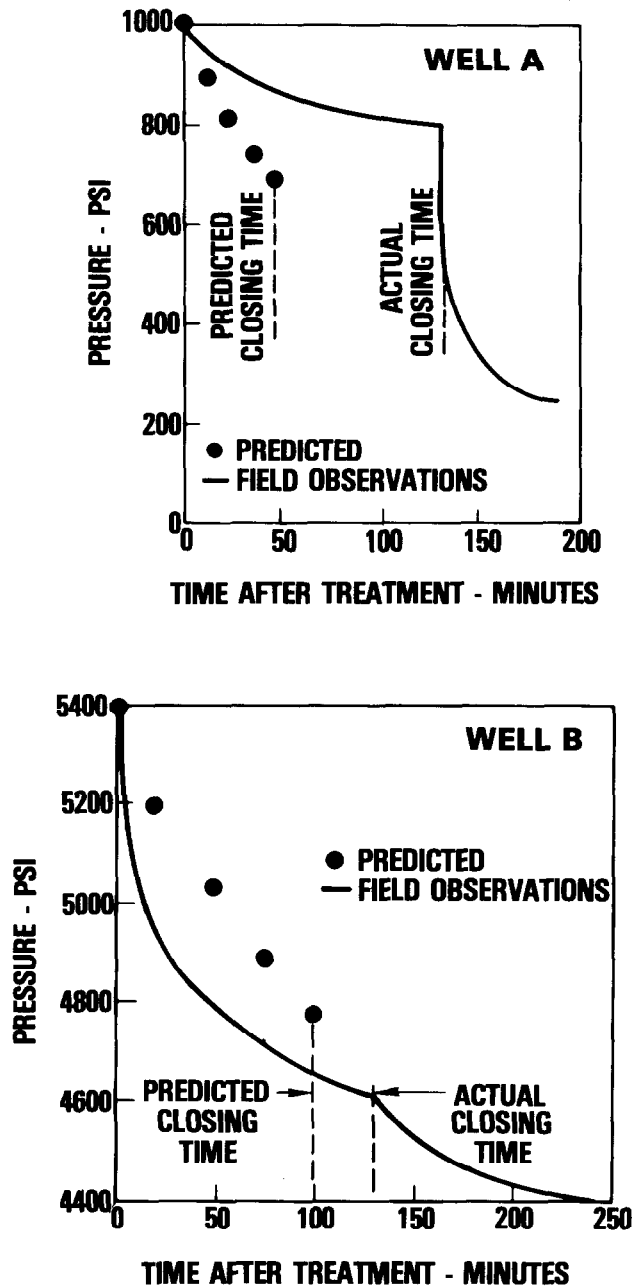


FIGURE 2—COMPARISON OF PREDICTED AND OBSERVED SURFACE TUBING PRESSURES DURING FRACTURE CLOSURE FOLLOWING HYDRAULIC FRACTURING TREATMENTS.

## COMPUTER MODEL

This section discusses the details of the computer model used to predict proppant transport both during and following hydraulic fracturing treatments. Any previous research utilized will not be detailed here. This section should give the reader a general idea of the complexity of predicting proppant transport and the various factors involved.

The first step in predicting proppant transport is to predict dynamic vertical fracture geometry, i.e., the geometry while injecting fluid and proppant. Because it is necessary to know the fracture length and width at various times, a numerical technique<sup>4</sup> was not feasible. (It was too time-consuming for the numerous calculations required.) For this reason the analytical model of Geertsma and de Klerk<sup>5</sup> was used. To insure consistency with the more accurate numerical method,<sup>4</sup> several internal checks were made so that at the end of the treatment the predicted dynamic fracture geometries were identical for both the analytical and numerical methods. For a wide variety of fracturing conditions, both methods predicted nearly identical fracture widths and lengths as functions of time.

The second major item that affects proppant transport is the loss of fluid to the formation as the proppant-fluid slurry flows along the fracture. This decreases the fluid velocity and increases the concentration of proppant. The change in concentration and fluid velocity can be obtained by a simple volume balance on the amount of fluid that enters a given fracture segment and the amount lost to the formation. Fluid loss can drag the fluid and proppant toward the fracture walls, but for most fracturing conditions, this effect is negligible.<sup>6</sup>

As fluid is injected into the fracture, the formation temperature near the wellbore decreases and fluid temperature increases. The prediction of this temperature variation of fracturing fluid with fracture length and time has been previously reported.<sup>7</sup> Example fluid temperature profiles are shown in Figure 3. The resulting temperature change alters the fluid loss and viscosity of the fluid, which in turn affects the settling velocity of the proppant.

The combination of fracture geometry, fluid loss, and fluid heating influences the settling velocity of the proppant-fluid slurry. Equations for calculating proppant settling are given in the next section. Ex-

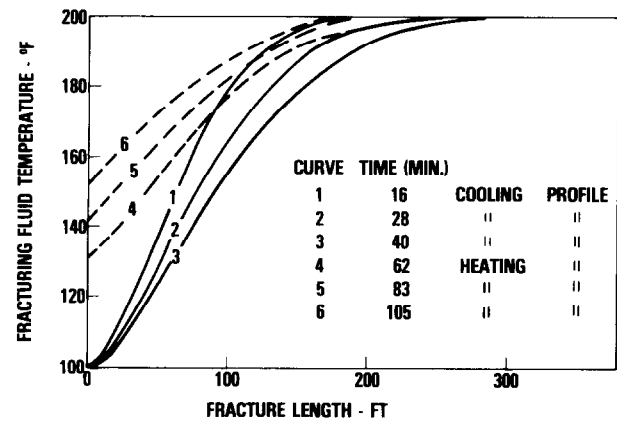


FIGURE 3—TEMPERATURE PROFILES OF FLUID IN A FRACTURE DURING AND FOLLOWING HYDRAULIC FRACTURING TREATMENT A IN FIGURE 1.

periments indicate that the proppant travels along the vertical fracture with the fluid. As the proppant settles, forming a proppant bank in the fracture, the cross-sectional area for flow decreases. This increases the fluid velocity in the fracture. Since the permeability of the proppant bank is much greater than the formation permeability, we assume that fluid loss occurs over the entire permeable reservoir sand even if it is covered by a proppant bank.

As the proppant bank continues to build, the velocity of the fluid across the top of the proppant bank may become so large that no more proppant can be deposited. In this case the proppant bank reaches an equilibrium height. The conditions required for an equilibrium bank height as reported by Babcock and Prokop<sup>8</sup> are used in this mathematical model.

Another factor influencing the flow of fluids in a fracture is the high-velocity jetting of the proppant-fluid slurry immediately after it passes through the perforations. Experiments in the laboratory have shown that this jetting is usually confined to a few feet of fracture near the wellbore. In the mathematical model presented here, we assume that the jetting effect is negligible and that the fracturing fluid flows through the perforations and expands over the entire fracture height in a short distance.

As soon as a fracturing treatment has been completed and the injection of fluid and proppant stops, the fracture begins to close. The force pushing the fracture closed is the minimum principal earth stress ( $S_0$ ), which acts against the fluid pressure in the fracture. The fracture closes as fluid is lost to

the permeable formation. The driving force for fluid loss is the pressure in the fracture minus the reservoir pressure ( $P_i - P_R$ ). The force holding the fracture open is the pressure in the fracture minus the minimum principal stress ( $P_i - S_o$ ). For a given increment of time ( $\Delta t$ ), an average fluid loss coefficient over the entire fracture is calculated and used to predict fluid loss for that increment of time. Then, from a volume balance, a new fracture volume and width ( $W_{i+1}$ ) can be calculated. From this new width, a new pressure in the fracture is obtained. This can be expressed as:

$$A = \frac{77.6 \bar{C} \Delta t H_n (S_o - P_i)}{W_{wb} H_g} \quad (1)$$

$$P_{i+1} = \frac{P_i (P_R - P_o) + A \cdot P_R}{P_R - P_o + A} \quad (2)$$

$$W_{i+1} = \frac{W_i (P_{i+1} - S_o)}{P_i - S_o} \quad (3)$$

(All terms are defined in the Nomenclature.) This procedure is repeated for as many time increments as required for the fracture to close.

While the fracture is closing, the temperature of the fracturing fluid increases because no more cool fluid is being injected. We found that for common fracturing conditions, an analytical solution could be used to approximate the heating of the fluid in the fracture. This analytical solution assumes that the temperature gradient into the formation is linear at the end of the treatment. This linear gradient is chosen such that the total energy of the system around the fracture is equal to the total energy calculated from a more accurate nonlinear temperature profile developed by Sinclair.<sup>7</sup> The results from the analytical solution were in good agreement with a numerical solution for the nonlinear temperature profiles. The temperature ( $T$ ) of the fluid at a given fracture length as a function of time is given by the following equation:

$$T = T_o + (T_R - T_o) \left\{ 1 - \operatorname{erf} \frac{a}{2 \sqrt{\kappa t}} - 2 \sqrt{\frac{\kappa t}{\pi a^2}} \left[ \exp \left( - \frac{a^2}{4 \kappa t} - 1 \right) \right] \right\} \quad (4)$$

Typical heating profiles are shown in Figure 3, along with the cooling profiles discussed above.

Once the fracture has completely closed on the proppant (and the final propped fracture geometry is obtained), the next step is to calculate a stimulation ratio. Normally, the shape of this fracture is irregular (as shown in Figure 1), so commonly used stimulation prediction methods are not applicable. An equation does exist for calculating stimulation for vertical fractures having a conductivity that varies with fracture length.<sup>9</sup> But, for the model presented here, the propped fracture height also varies with fracture length. Simple elasticity theory predicts that a short distance away from a propped bank, an unpropped portion of the fracture will close completely. Here we assume that only those portions of the fracture that contain proppant remain open.

A study using a three-dimensional reservoir simulator<sup>2</sup> determined that only that portion of the propped fracture height which is directly opposite the net productive reservoir sand contributes to stimulation. Thus the gross fracture height used in calculating fracture conductivity can at most be equal to the net reservoir thickness. If the propped fracture height is less than the net reservoir sand thickness, the conductivity ratio must be reduced by  $H_g/H_n$ . This result is similar to that reported by Tinsley.<sup>10</sup> Using this information we can calculate a stimulation ratio ( $J/J_o$ ) from the following equation, which was developed from Raymond and Binder:<sup>9</sup>

$$J/J_o = \frac{\ln (r_e/r_w)}{\left\{ \sum_{i=1}^N \ln \left[ \frac{30.5 \pi L_i + W k_f H_e / H_n k}{30.5 \pi L_{i-1} + W k_f H_e / H_n k} \right] \right\} + \ln (r_e/L_N)} \quad (5)$$

Note that  $W$ ,  $k_r$ , and  $H_e$  are evaluated at a distance  $L_i$  from the wellbore, where  $i=1,2,3\dots N$ . The effective fracture height ( $H_e$ ) is that propped portion opposite the net permeable reservoir sand. If the proppant settles below the net reservoir sand, then the fracture closes completely and the conductivity ratio ( $W k_r H_e / k H_n$ ) in this portion of the fracture is zero. For gas wells, the effect of turbulence both in the formation and in the fracture is considered.

Due to the complexity of the mathematical model, it is impossible to check calculations by hand. But several internal checks are made to assure the reliability of the model. For example, the amount of proppant in the fracture after the treat-

ment and the amount of proppant injected are both calculated and found to agree within a few percent. Also, propped fracture geometries calculated using 50 time increments per treatment and 100 time increments per treatment give the same results. For this reason, 50 time increments are used during the proppant injection portion of the treatment. Fracture closure is calculated with additional time steps.

### SETTLING: THEORY AND EXPERIMENTS

This section discusses the theory and experimental verification of proppant settling. Since proppant settling is a complicated phenomenon, the effects of non-Newtonian fluids, fracture walls, and concentrated slurries will be discussed separately.

#### Single Particle in a Newtonian Fluid

For a single particle in a Newtonian fluid, the terminal settling velocity can be calculated by equating the drag force ( $\pi C_D V^2 \rho d^2 / 8$ ) and the gravitational, minus buoyant forces ( $\pi d^3 g(\rho_p - \rho) / 6$ ) on the particle. For spheres, the drag coefficient is a function of the Reynolds number and can be closely approximated using three different regions of Reynolds numbers. From this, the settling velocity of a single sphere in a Newtonian fluid with no walls present to hinder the settling can be given by the following equations:

For  $N_{Re} \leq 2$  (Stokes-law region),

$$C_D = 24/N_{Re} \text{ and } V_\infty = \frac{g(\rho_p - \rho)d^2}{18\mu} \quad (6a)$$

For  $2 < N_{Re} < 500$  (intermediate region),

$$C_D = 18.5/N_{Re}^{0.6} \text{ and } V_\infty = \frac{20.34(\rho_p - \rho)^{0.71} d^{1.14}}{\rho^{0.29} \mu^{0.43}} \quad (6b)$$

For  $N_{Re} \geq 500$  (Newton's-law region),  $C_D = 0.44$

$$\text{and } V_\infty = 1.74 \sqrt{\frac{g(\rho_p - \rho)d}{\rho}} \quad (6c)$$

If the flow around the particle is laminar, the equations will hold even if the particle is not perfectly spherical. This has been verified in this study as well as in previous research.<sup>11</sup> For most

proppants, settling is in the Stokes region. However, serious errors in predicting settling velocity can be made if Eq. (6a) is used when  $N_{Re} \gg 2$ .

#### Non-Newtonian Fluids

For non-Newtonian fluids, the fluid viscosity varies with shear rate. If settling is in a stagnant, non-Newtonian fluid, the effective shear rate on the particle is the settling velocity divided by the particle diameter ( $V/d$ ).<sup>12</sup> If this shear rate is used to calculate the fluid viscosity with a power-law fluid model ( $\mu = K\dot{\gamma}^{n-1}$ ), Stokes' law for settling velocity can be predicted by

$$V_\infty = \left[ \frac{g(\rho_p - \rho)d}{18K} \right]^{1/n} d \quad (7)$$

Settling velocity is a function of  $K$  and  $n$ , the power law parameters. For non-Newtonian fluids, the settling velocity is proportional to  $d^{(1+n)/n}$  instead of  $d^2$  as for Newtonian fluids. This effect can be seen in Figure 4, where settling velocities of different diameter proppants are plotted. The theoretical

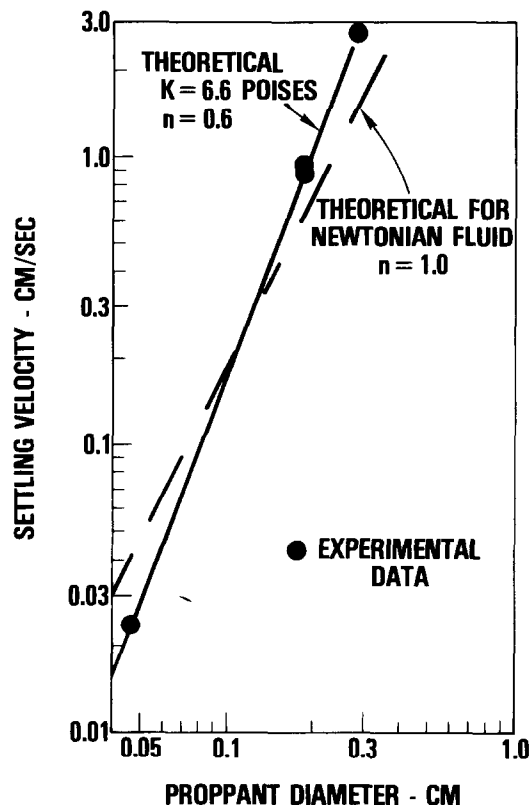


FIGURE 4—THEORETICAL AND EXPERIMENTAL PROPPANT SETTLING VELOCITIES IN NON-NEWTONIAN FLUIDS DIFFER FROM NEWTONIAN PREDICTIONS.

(solid) line for a non-Newtonian fluid with  $n = 0.6$  fits the experimental data quite well, whereas the Newtonian (dashed) line does not fit the data.

For non-Newtonian fluids, the intermediate region, Eq. (6b), cannot be solved explicitly. The solution becomes trial-and-error, using a non-Newtonian viscosity—which is a function of the settling velocity. For the Newton's-law region, settling velocity is not a function of the viscosity and Eq. (6c) is valid. For most fracturing conditions, settling Reynolds numbers are low and Eq. (7) can be used.

A further complication arises for flowing non-Newtonian fluids, because there will be a shear rate imposed on the proppant in the direction of fluid motion (as well as a shear rate due to the particle settling). To determine the importance of this effect, experiments with single particles were performed in an apparatus composed of concentric cylinders approximately 1 ft in diameter and 3 ft high. The gap between the cylinders was varied from 1/4 in. to 3/4 in. The inner cylinder was rotated so that a shear rate was imposed on the fluid contained in the annulus. For this geometry, the shear rate between the cylinders is constant throughout the gap.

For Newtonian fluids, the shear rate imposed on the particles did not affect the settling velocity of the proppant. This was expected since Newtonian fluid viscosity is constant with shear rate. However, when non-Newtonian fluids were used, proppants settled faster when the fluid was sheared than when the fluid was stagnant.

The effective shear rate on a proppant particle was found to be the vector sum of the shear rate due to proppant settling ( $V/d$ ) and the shear rate imposed by fluid motion ( $\dot{\gamma}_1$ ), i.e.,

$$\dot{\gamma} = \sqrt{\left(\frac{V}{d}\right)^2 + \dot{\gamma}_1^2} \quad (8)$$

For Stokes' law the settling velocity can be calculated from

$$V_o = \frac{980 (\rho_p - \rho)d^2}{18K} \left[ \left(\frac{V_o}{d}\right)^2 + \dot{\gamma}_1^2 \right]^{1/n} \quad (9)$$

Settling velocity cannot be expressed explicitly, so a trial-and-error solution is required.

In Figure 5, settling velocity is plotted as a function of shear rate for four proppant diameters. The curves were calculated from Eq. (9). Although the data (measured with the concentric cylinder ap-

paratus) do not lie exactly on the curves, the trend is similar. For the smallest particles, there was a 40-fold increase in settling velocity when the imposed shear rate on the particle was increased from 0 to 90  $\text{sec}^{-1}$ . For the largest particle, this effect was only about 6-fold at the maximum shear rate.

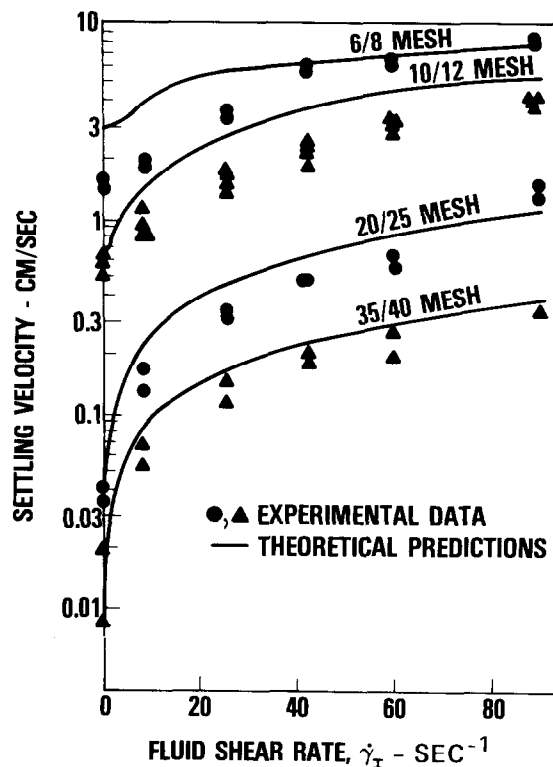


FIGURE 5—SHEARING A NON-NEWTONIAN FLUID INCREASES PROPPANT SETTLING VELOCITY IN A FLUID WITH  $n = 0.35$ ,  $K = 9.0$  POISES. THE PROPPANTS ARE SAND AND GLASS BEADS.

In a fracture, fluid velocity varies from zero at the walls to a maximum midway between the walls. For a power-law fluid, the velocity profile is

$$U = \bar{U} \left( \frac{2n+1}{n+1} \right) \left[ 1 - \left( \frac{y}{W/2} \right)^{\frac{n+1}{n}} \right] \quad (10)$$

The shear rate ( $\dot{\gamma}_1$ ) is zero in the center of the fracture and a maximum at the walls. From the definition of  $\dot{\gamma}_1 = -dU/dy$ ,

$$\dot{\gamma}_1 = \frac{2\bar{U}}{W} \left( \frac{2n+1}{n} \right) \left( \frac{y}{W/2} \right)^{1/n} \quad (11)$$

The value of  $\dot{\gamma}_1$  in fracture flow is a function of  $y$ —the location between the fracture walls.

Proppants traveling midway between the fracture walls will have  $\dot{\gamma}_I = 0$  and should settle as in a stagnant fluid. Proppants close to the walls will be influenced by  $\dot{\gamma}_I$ , however, and in non-Newtonian fluids should settle faster than in a stagnant fluid.

Single particle settling velocities were measured in a vertical lucite fracture 8 ft long and 1.5 ft high, with a variable width of 1/8 and 1/2 in. For Newtonian and slightly non-Newtonian ( $0.8 < n < 1.0$ ) fluids, proppants traveled midway between the fracture walls and settled as in a stagnant fluid.

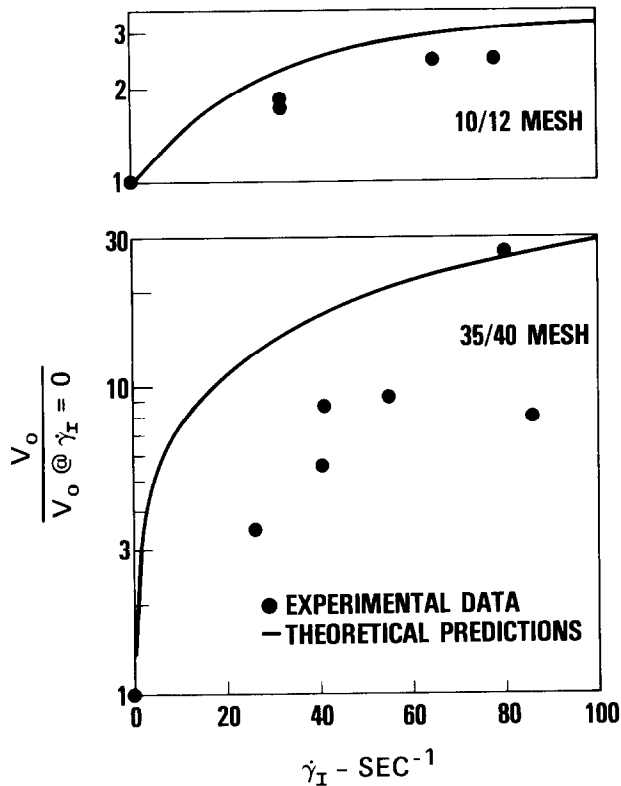


FIGURE 6—FLOW IN A 1/2-IN. WIDE FRACTURE INCREASES PROPPANT SETTLING VELOCITY IN A FLUID WITH  $n=0.4$ ,  $K = 6.0$  POISES. THE PROPPANTS ARE SAND AND GLASS BEADS.

In highly non-Newtonian fluids ( $0.34 < n < 0.4$ ), proppants settled much faster when the fluid was flowing, as shown in Figures 6 and 7. Here it was assumed that the proppant traveled with the fluid in the horizontal direction at a velocity  $U$ . From this and Eq. (10), the position of the proppant between the fracture walls ( $y$ ) could be obtained. The imposed shear rate at this point was then calculated from Eq. (11). The proppants migrated away from

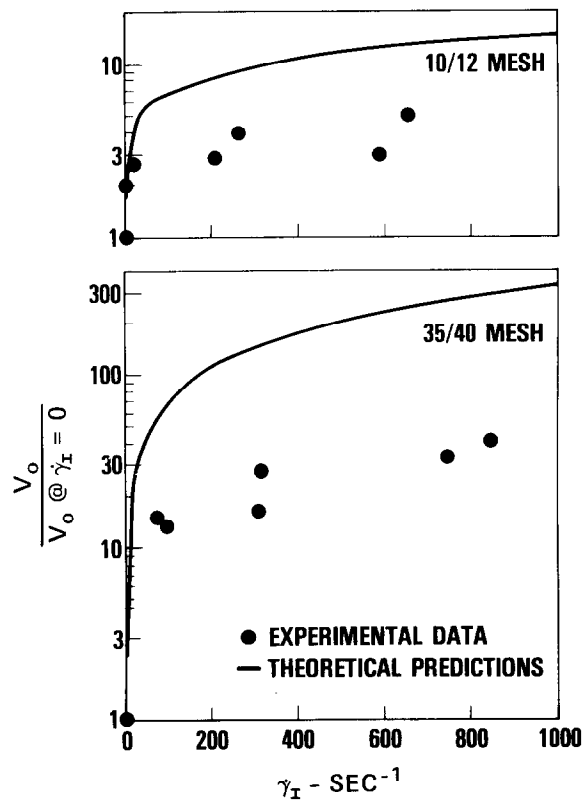


FIGURE 7—FLOW IN A 1/8-IN. WIDE FRACTURE INCREASES PROPPANT SETTLING VELOCITY IN A FLUID WITH  $n=0.35$ ,  $K = 7.0$  POISES. THE PROPPANTS ARE SAND AND GLASS BEADS.

the fracture center and traveled near the fracture walls. This migration of particles toward the walls was also reported in flow of non-Newtonian fluids in tubes.<sup>13</sup> Even though the effect of flow was not as great as predicted, the 35/40 mesh proppant settled 20 to 40 times faster at the higher shear rates than it did when the fluid was stagnant. Flow rate at these high shear rates is equivalent to 0.15 BPM/ft of fracture height for one fracture wing, a flow rate in the range of normal field values.

In summary, settling velocities measured in stagnant non-Newtonian fluids are not reliable for predicting proppant transport in flow. Settling must be determined as a function of the fluid shear rate. Proppants that are completely suspended in a stagnant, highly non-Newtonian fluid will settle when the fluid is sheared.

#### Wall Effects

When particles are flowing through a fracture, the presence of the fracture walls near the particle

hinders settling. There have been many attempts to theoretically determine this wall effect.<sup>14-18</sup> This study found that the following equation<sup>14</sup> is valid for vertical fractures when  $N_{Re} \leq 1$ :

$$f_w = \frac{V_o}{V_\infty} = 1 - 0.6526(d/W) + 0.147(d/W)^3 - 0.131(d/W)^4 - 0.0644(d/W)^5 \quad (12a)$$

However, when  $N_{Re} \geq 100$ ,

another equation must be used<sup>17</sup>

$$f_w = \frac{V_o}{V_\infty} = 1 - \left[\frac{d}{2w}\right]^{3/2} \quad (12b)$$

Between these two regions, a simple linear interpolation based on the Reynolds number is used. For most cases,  $N_{Re} < 1$  and Eq. (12a) is applicable.

Figure 8 shows that Eq. (12a) for a non-Newtonian fluid agrees well with experimental data. Data in the laboratory were obtained using various proppants, fluids, smooth-wall lucite fractures, and rough-walled fractures made by fracturing carbonate rock. Fracture widths of 1/8, 1/4, and 3/4 in. were used. The roughness of the carbonate fractures did not affect settling velocity other than the presence of a narrow gap as predicted by Eqs. (12a) and (12b).

#### Concentrated Slurries

In fracturing treatments, proppants are usually injected at a concentration of around 2 to 3 lb/gal. As fluid is lost to the formation, however, the concentration increases and can become quite high. The settling of particles in slurries is a different phenomenon than the settling of single particles. Several theories are available on the settling of concentrated slurries, but only a few are substantiated by experimental data.<sup>19,20</sup> These previous endeavors showed that the settling velocity ( $V$ ) of particles in a slurry is proportional to  $\phi^{5.5}$ , where  $\phi$  = slurry porosity, for Newtonian fluids having a low Reynolds number and concentrations from 3 up to 20 lb/gal.

One theory<sup>20</sup> explained that concentrated slurries increase the fluid density, which the proppant "senses" as it settles. Also, the slurry viscosity is increased by a factor of  $\phi^{3.5}$ . Finally, the relative velocity past the proppant is increased by  $\phi$ , which

● EXPERIMENTAL DATA  
— THEORETICAL FOR  $n=0.64$   
K=3.4 POISES

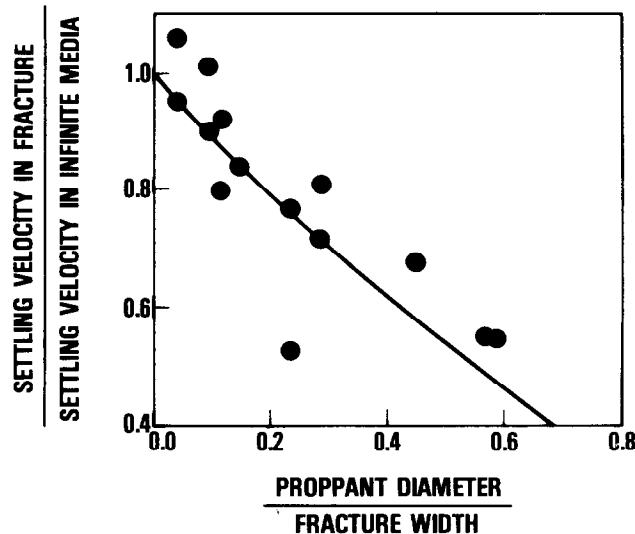


FIGURE 8--THE PRESENCE OF FRACTURE WALLS HINDERS PROPPANT SETTLING.

increases the drag force on the proppant and decreases the settling velocity. Using all these factors in the Newtonian Eqs. (6a)-(6c), we can summarize the concentration effect:

For  $N_{Re} \leq 2$

$$V/V_o = \phi^{5.5} \quad (13a)$$

For  $2 < N_{Re} < 500$

$$V/V_o = \phi^{3.5} \quad (13b)$$

For  $N_{Re} \geq 500$

$$V/V_o = \phi^2 \quad (13c)$$

In Figure 9, experimentally determined exponents on the porosity are plotted as a function of Reynolds number. There is good agreement between the theoretical prediction (Eq. (13a)-(13c)) and the experimental data, which were taken in water and in a 35 centipoise oil in the geometries described below. Note that a better prediction is obtained if a logarithmic linear interpolation between Reynolds numbers of 2 and 500 is used. For most fracturing treatments,  $N_{Re} < 2$  and Eq. (13a) will be valid.

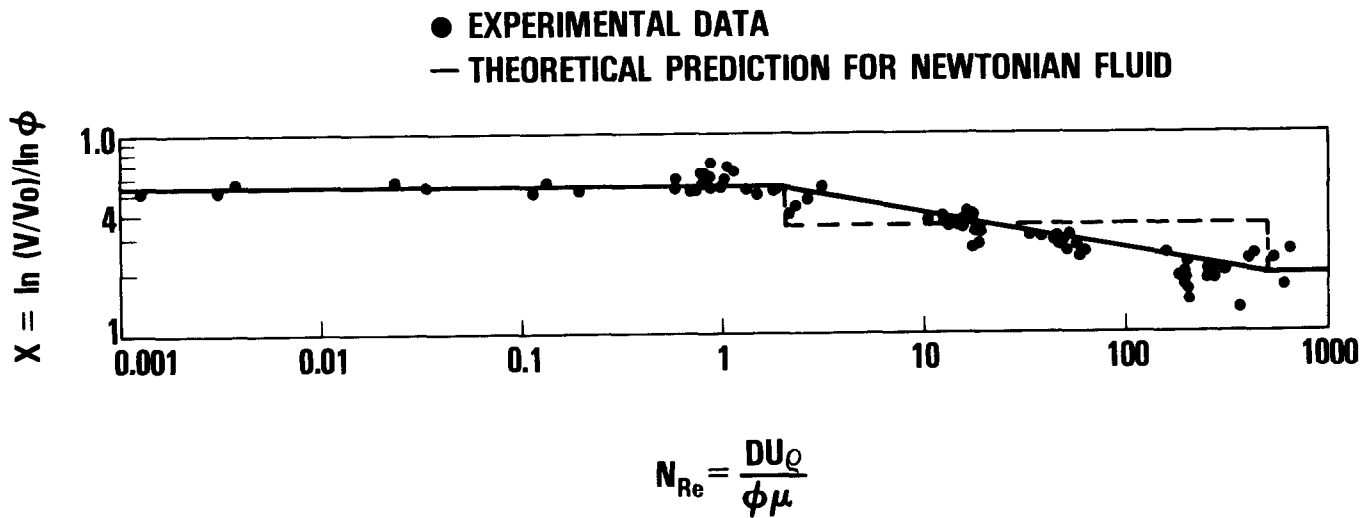


FIGURE 9—THE EFFECT OF CONCENTRATION ON THE SETTLING OF PROPPANT-FLUID SLURRIES DEPENDS ON THE REYNOLDS NUMBER.

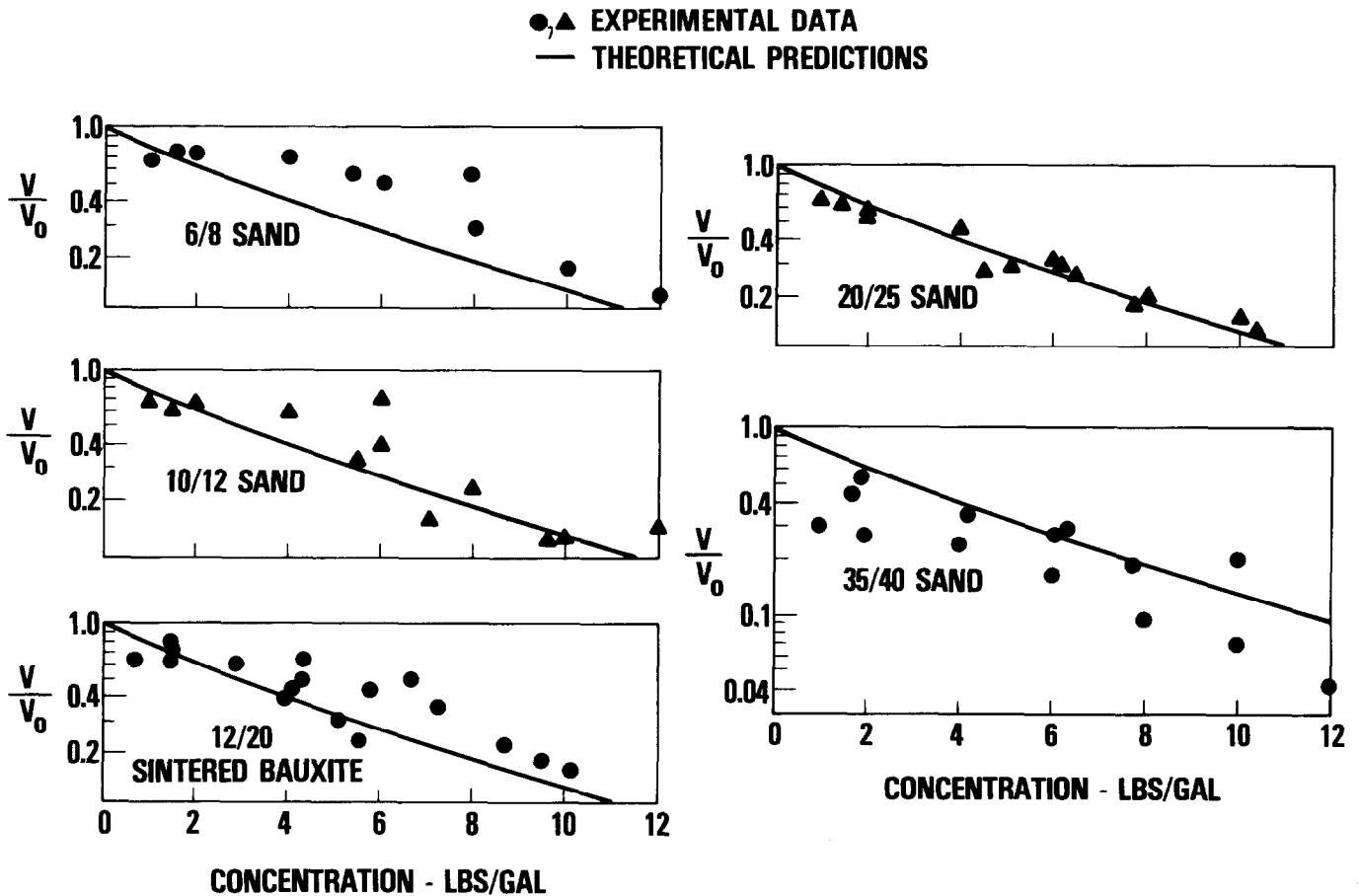


FIGURE 10—PROPPANT-FLUID SLURRY SETTLING VELOCITY DECREASES WITH PROPPANT CONCENTRATION IN A NON-NEWTONIAN POLYACRYLAMIDE SOLUTION WITH  $n=0.75$ ,  $K=5.5$  POISES.

To see if these data are also applicable for non-Newtonian fluids, we measured settling velocities for different slurries in 2-3/8-in. diameter cylinders, 1/8-in.-wide fractures, and 1/2-in.-wide fractures. Data are shown in Figure 10 for one of these fluids—a polyacrylamide solution with  $n = 0.75$  and  $K = 5.5$  poises. There is good agreement between the predicted and observed results for this non-Newtonian fluid. It appears that the concentrated slurry correction is valid for non-Newtonian fluids. In Figure 10, the sintered bauxite concentrations were altered so that at a given concentration the slurry porosity was the same as it would be for a sand slurry of that concentration. That is, the concentration of the sintered bauxite proppant was reduced by a factor of sand density/sintered bauxite density =  $2.65/3.65$ . These measurements were made in vertical fractures with stagnant fluids and would apply directly to settling while the fracture is closing.

The effect of concentration can be quite large. For an 11-lb/gal slurry, there is approximately a 10-fold reduction in settling velocity (as compared to a single particle in the fluid). Although proppants are not injected at this high concentration, concentration increases as the proppant-fluid slurry flows along a fracture and concentrations can reach 11 lb/gal. When the fracture closes, concentrations often reach the settled bank concentration, which is 35 lb/gal for sand.

Currently we are measuring settling velocities of proppant-fluid slurries flowing through fractures. It was found that in some cases proppants agglomerate or cluster together, which can affect proppant settling. We intend to quantify this clustering phenomenon before completion of this research.

## CONCLUSIONS

1. Proppant transport is a complex phenomenon that cannot be adequately described mathematically unless several important parameters are appropriately taken into account. Numerical and computer techniques must be used to obtain accurate proppant transport predictions.
2. Proppant settling during the time required for fracture closure after a hydraulic fracturing treatment can have an important bearing

on the distribution of proppant in the fracture and may determine the success or failure of a treatment.

3. Stimulation resulting from proppant fracturing treatments is a function of the position of the propped portion of the fracture relative to the permeable reservoir rock. Only those reservoir rock portions which are actually opposite the propped fracture will be stimulated.
4. The most important variables affecting proppant settling are the non-Newtonian characteristics of the fluid, the presence of fracture walls, the concentration of proppant, and the shearing of non-Newtonian fluids. All these factors must be considered to accurately predict proppant transport.

## NOMENCLATURE

- $A$  = intermediate variable for use in closing calculations in Eq. (1), dimensionless
- $a$  = distance where the linear temperature profile from the fracture into the formation reaches  $T_R$ , ft (used in Eq. (4))
- $\bar{C}$  = average fluid loss coefficient,  $\text{ft}/\sqrt{\text{Min}}$
- $C_D$  = drag coefficient on a sphere, dimensionless
- $d$  = proppant diameter, cm
- $f_w$  = wall factor, a function of Reynolds' number (Eqs. (12a) and (12b)), dimensionless
- $g$  = gravitational constant =  $980 \text{ cm}/\text{sec}^2$
- $H_e$  = effective propped fracture height, ft
- $H_g$  = total fracture height, ft
- $H_n$  = height of net permeable reservoir sand, ft
- $K$  = consistency index for power-law fluid, poises
- $k$  = formation permeability, md
- $k_f$  = proppant permeability in a fracture, md
- $L_o$  = first increment of fracture length =  $r_w$ , ft
- $L_i$  =  $i$  th fracture length distance, ft

$L_N$  = total propped fracture length, ft  
 $N_{Re}$  = settling Reynolds number =  $dV\rho/\mu\phi$ , dimensionless  
 $n$  = power-law index, dimensionless  
 $P_i$  = average pressure in the fracture at the start of a closing time step, psi  
 $P_{i+1}$  = averaged pressure in the fracture at the end of a closing time step, psi  
 $P_o$  = average pressure in the fracture immediately following completion of the fracturing treatment, psi  
 $P_R$  = reservoir pressure, psi  
 $r_c$  = drainage radius of well, ft  
 $r_w$  = wellbore radius, ft  
 $S_o$  = minimum principal earth stress which must be overcome to create a fracture, psi  
 $T$  = temperature in fracture at a given length at any time, °F  
 $T_o$  = temperature in fracture at a given length immediately following completion of fracturing treatment, °F  
 $T_R$  = reservoir temperature, °F  
 $t$  = time, min  
 $U$  = fluid velocity in a fracture at position  $y$ , cm/sec  
 $\bar{U}$  = bulk average fluid velocity in a fracture, cm/sec  
 $V$  = settling velocity of proppant, cm/sec  
 $V_\infty$  = settling velocity of a single proppant particle in an infinite media, cm/sec  
 $V_o$  = settling velocity of a single proppant particle in a given configuration (as opposed to a concentrated slurry of proppant), cm/sec  
 $W$  = fracture width, cm  
 $W_i$  = fracture width at a given length at the start of a closing time step, cm  
 $W_{i+1}$  = fracture width at a given length at the end of a closing time step, cm

$W_{wb}$  = fracture width at the wellbore, cm  
 $y$  = position between fracture walls measured from center, cm ( $y = 0$  at center,  $y = W/2$  at walls)  
 $\dot{\gamma}$  = total effective shear rate on proppant,  $\text{sec}^{-1}$   
 $\dot{\gamma}_1$  = shear rate imposed on proppant by fluid,  $\text{sec}^{-1}$   
 $\phi$  = porosity of a proppant-fluid slurry, fraction  
 $\mu$  = viscosity, poises (for non-Newtonian fluids  $\mu = K\dot{\gamma}^{n-1}$ )  
 $k$  = thermal diffusivity (thermal conductivity/specific heat capacity),  $\text{ft}^2/\text{min}$   
 $\rho$  = density of fluid, gm/cc  
 $\rho_p$  = proppant density, gm/cc

## REFERENCES

1. Daneshy, A. A.: "Numerical Solution of Sand Transport in Hydraulic Fracturing," Paper SPE 5636 presented at SPE 50th Annual Fall Meeting, Dallas, Sept. 28-Oct. 1, 1975.
2. Spillette, A. G., Hillestad, J. G. and Stone, H. L.: "A High-Stability Sequential Solution Approach to Reservoir Simulation," Paper SPE 4542 presented at SPE 48th Annual Fall Meeting, Las Vegas, Nev., Sept. 30 - Oct. 3, 1973.
3. McGuire, W. J. and Sikora, V. J.: "The Effect of Vertical Fractures on Well Productivity," *Petroleum Transactions*, AIME, 219 (1960) 401-403.
4. Kiel, O. M.: "A New Hydraulic Fracturing Process," *J. Pet. Tech.* (Jan. 1970) 89-96.
5. Geertsma, J. and de Klerk, F.: "A Rapid Method of Predicting Width and Extent of Hydraulically Induced Fractures," *J. Pet. Tech.* (Dec. 1969) 1571-81.
6. Terrill, R. M.: "Laminar Flow in a Uniformly Porous Channel," *The Aeronautical Quarterly*, 15 (August 1965) 299-310.
7. Sinclair, A. R.: "The Effects of Heat Transfer in Deep Well Fracturing," *J. Pet. Tech.* (Dec. 1971) 1484-92.
8. Babcock, R. E., Prokop, C. L., and Kehle, R. O.: "Distribution of Propping Agents in Vertical Fractures," *Producers Monthly* (November 1967) 11-18.
9. Raymond, L. R. and Binder, G. G., Jr.: "Productivity of Wells in Vertically Fractured, Damaged Formations," *J. Pet. Tech.* (January 1967) 120-130.
10. Tinsley, J. M., et al.: "Vertical Fracture Height - Its Effect on Steady - State Production Increase," Paper SPE 1900 presented at SPE 42nd Annual Fall Meeting, Houston, Oct. 1-4, 1967.

11. Achenbach, E.: "The Effects of Surface Roughness and Tunnel Blockage on the Flow Past Spheres," *J. Fluid Mech.*, 65 (1974) 113-125.
12. Slattery, J. C. and Byrd, R. B.: "Non-Newtonian Flow Past a Sphere," *Chem. Eng. Sci.*, 16 (1961) 231-241.
13. Gauthier, F., Goldsmith, H. L. and Mason, S. G.: "Particle Motions in Non-Newtonian Media. II. Poiseuille Flow," *Trans. Soc. Rheology*, 15 (1971) 297-330.
14. Happel, J. and Brenner, H.: *Low Reynolds Number Hydrodynamics*, Prentice-Hall Inc., Englewood Cliffs, N. J. (1965) 322-357.
15. Fidleris, V. and Whitmore, R. L.: "Experimental Determination of the Wall Effect for Spheres Falling Axially in Cylindrical Vessels," *Brit. J. Appl. Phys.*, 12 (Sept. 1961) 490-494.
16. Francis, A. W.: "Wall Effect in the Falling-Ball Method for Viscosity," *Physics*, 4 (1933) 403-6.
17. Munroe, H. S.: *Trans.*, AIME, 17 (1888) 637.
18. Sutterby, J. L.: "Falling Sphere Viscometry. I. Wall and Inertial Corrections to Stokes Law in Long Tubes," *Trans. Soc. Rheology*, 17 (1973) 559-573.
19. Steinour, H. H.: "Rate of Sedimentation. Nonflocculated Suspensions of Uniform Spheres," *Ind. Eng. Chem.*, 36 (1944) 618-24.
20. Richardson, J. F. and Zaki, W. N.: "The Sedimentation of a Suspension of Uniform Spheres Under Condition of Viscous Flow," *Chem. Eng. Sci.*, 3 (1954) 65-73.

#### ACKNOWLEDGMENTS

I wish to thank Exxon Production Research Company for permission to publish this paper. Special thanks are due to A. E. Cowan, A. D. Sheno, E. T. Rinche, and D. J. Broussard, who performed the experiments discussed in this paper.